Raman scattering and phase transitions in $(NH_4)_3TiF_7$

Yu. V. Gerasimova,[a,b]* A. S. Oreshonkov,[a,b] N. M. Laptash,[c] A. S. Krylov,[a] A. R. Aliev [d] and E. M. Roginsky [e,f]

[a]Kirensky Institute of Physics, Federal Research Center KSC SB RAS, 660036 Krasnoyarsk, Russia

[b]Institute of Engineering Physics and Radio Electronics, Siberian Federal University, 660079 Krasnoyarsk, Russia

[c]Institute of Chemistry, Far Eastern Branch of RAS, 690022 Vladivostok, Russia

[d]Amirkhanov Institute of Physics, Dagestan Scientific Center of RAS, 367003 Makhachkala, Russia

[e]Ioffe Physical Technical Institute, Russian Academy of Sciences, 194021 St.-Petersburg, Russia

[f]St.-Petersburg State University, 199034 St.-Petersburg, Russia

E-mail: jul@iph.krasn.ru

Raman spectra of $(NH_4)_3TiF_7$ in a wide range of frequencies (20–3400 cm^{-1}) and temperatures (8–370 K) including two phase transitions are obtained. which are accompanied by symmetry increase at temperature decrease. First principles calculations of lattice dynamics and assignment of the observed lines to specific vibrational types are performed. An unusual reconstructive phase transition accompanied by an increase in the symmetry (P4/mnc→$Pa\overline{3}$) with decreasing temperature is reflected by the emergence of a large number of vibrational lines in the Raman spectra at low temperatures meaning ordering of TiF_6 octahedra and symmetry lowering of NH_4 tetrahedra. The unique band at 97 cm^{-1} (mixed translational (NH_4+F7) vibration) indicates the enhancement of the hydrogen bond between ammonium group and the free fluorine atom in the structure of double salt.

Introduction

Titanium fluoride double salt $(NH_4)_3TiF_7 = (NH_4)_2TiF_6 \cdot NH_4F = (NH_4)_3[TiF_6]F$ is the main product of fluoride processing of titanium-containing raw materials (ilmenite, rutile) when ammonium hydrogen difluoride (NH_4HF_2) is used as fluorinating agent to produce pigmentary titanium dioxide (TiO_2).[1–5] Marignac was the first who described this compound back in 1859.[6] Only recently its crystal structure was studied by Molokeev *et al.*[7] The compound crystallizes in tetragonal syngony (space group *P*4/*mnc*) at room temperature. The crystal structure incorporates three independent TiF_6 octahedra, one of them, $Ti3F_6$ is disordered among four positions. The disordering looks like the gyration of the pseudo-threefold axis of the octahedron $Ti3F_6$ around the fourfold axis of the crystal. Two independent ammonium ions are coordinated by two and three TiF_6 polyhedra.

Optical and differential scanning calorimetric (DSC) investigations have shown that $(NH_4)_3TiF_7$ undergoes two reversible first order structural transformations.[8] An unusual succession of two structural phase transitions was observed upon heating and cooling

$$P4/mbm \xleftrightarrow{361\,K} P4/mnc \xleftrightarrow{293\,K} Pa\overline{3}.$$ Maxima of the heat capacity peaks were located at the temperatures $T_1 = 361\pm2.0$ K and $T_2 = 293\pm1.0$ K. The sum of entropies associated with both phase transitions is rather large: $\Sigma\Delta S_i = \Delta S_1 + \Delta S_2 = 32\pm2$ J/mol K.[9] Individual values of entropy change in $(NH_4)_3TiF_7$ differ from each other significantly: $\Delta S_1 = 9.2\pm0.6$ J/(mol K) ($\sim R\ln3$), $\Delta S_2 = 22.7\pm1.6$ J/(mol K) ($\sim R\ln16$). The very large ΔS_2 value is the result of large atomic displacements in the reconstructive transformation. Moreover, the phase transition at T_2 was accompanied by the reversible cracking of crystals observed in polarizing-optic measurements, which allowed it to be considered a reconstructive transformation.[8] During such trans-

formation, total restructuring of hydrogen bonds occurs. Breaking of hydrogen bonds and creating new ones take place.[7]

The aim of the current study is to investigate the unusual reconstructive phase transition in the $(NH_4)_3TiF_7$ crystal using Raman spectroscopy.

Experimental

Synthesis

The starting substances for the synthesis of $(NH_4)_3TiF_7$ were solid $(NH_4)_2TiF_6$ and concentrated solution of NH_4F (40 wt %) of a reagent grade. The threefold excess of NH_4F was used relative to the reaction: $(NH_4)_2TiF_6 + NH_4F = (NH_4)_3TiF_7$. 10–11 g of $(NH_4)_2TiF_6$ were added to 50 ml of hot solution of NH_4F (pH ~ 7–8). Upon cooling to room temperature, a polycrystalline precipitate of titanium fluoride double salt was obtained, which was filtered, washed with cold water and alcohol and air dried. From the mother liquor, transparent single crystals of $(NH_4)_3TiF_7$ in the form of tetragonal prisms or cubes were formed, which were also used for Raman experiments.

Spectral acquisition

The unpolarized Raman spectra were collected in a backscattering geometry, using a triple monochromator Horiba Jobin Yvon T64000 Raman spectrometer operating in double subtractive mode, and detected by a LN-cooled charge-coupled device. The spectral resolution for the recorded Stokes side Raman spectra was set to ~4 cm^{-1} (this resolution was achieved with 1800 grooves/mm gratings and 100 mm slits). The microscope system based on Olympus BX41 microscope with an Olympus 50x objective lens $f = 0.8$ mm with NA = 0.75 numerical aperture provides a focal spot diameter of about 2 μm on the sample. Single-mode argon 514.5 nm from a Spectra-Physics Stabilite 2017 Ar$^+$ laser of 5 mW on the sample was used as excitation light source. The intensity of the laser light was adjusted to avoid sample heating.

DFT calculations

To interpret the observed Raman spectra, quantum chemical calculation of the structure and vibrational spectra of the low temperature phase of $(NH_4)_3TiF_7$ at density functional theory (DFT) level using CASTEP program package were made.[10] Initial structure of the low temperature cubic phase $Pa\overline{3}$ was completely optimized using either local density approximation (LDA)[11] or generalized gradient approximation (GGA) with PBE exchange functional.[12] Calculations were carried out using norm-conserving pseudopotentials for electronic configurations $1s^1$ (hydrogen), $2s^22p^3$ (nitrogen), $2s^22p^5$ (fluorine) and $3s^23p^63d^24s^2$ (titanium). Optimization of intracell atomic positions was carried out under following convergence limits: $5.0\ 10^{-8}$ eV per atom for energy, 0.01 eV/Å for forces, 0.02 GPa for compression, and $5.0\ 10^{-4}$ Å for displacement. The value of limiting cutoff of plane waves Ecut was chosen to be 1000 eV. Integration over the Brillouin zone was done by the method of special points [13] on 2×2×2 and 3×3×3 grids. Phonon spectrum was calculated using perturbation theory of density functional (DFPT).

Results and discussion

Raman spectra of $(NH_4)_3TiF_7$ in the range of vibrational frequences of the TiF_6 octahedral group recorded at different temperatures are presented in Fig. 1. The Raman intensity maps and temperature transformation of internal bending and stretching vibrations of ammonium ions are shown in Figs 2 and 3, respectively.

The lattice parameter of $(NH_4)_3TiF_7$ structure optimized using LDA approximation (11.414264 Å) is 3.1 % lower, while that obtained using GGA (PBE) approximation (12.104707 Å) is 2.73 % larger, than the experimentally measured value at 143 K (11.78287 Å),[7] which is in agreement with the general tendency that LDA underestimates, while GGA (PBE) overestimates lattice parameters.[14]. Calculation of phonon energies using both LDA and GGA approximations revealed no modes with imaginary frequencies, which evidences the stability of $Pa\overline{3}$ structure down to 0 K. Calculated phonon spectrum in the range 1350–1700 cm^{-1} corresponds to

the bending NH_4 vibrations, and the 2570–3260 cm^{-1} range contains stretching vibrations of N–H bonds. Internal vibrations of TiF_6 octahedra are located in the range below 650 cm^{-1}.

Lattice modifications connected with phase transitions are well pronounced in experimental Raman spectra. Vibrational frequencies observed at different temperatures together with their assignments are listed in Table 1.

Crystal structure data for both room temperature and low temperature phases of $(NH_4)_3TiF_7$[7] should be used for more detailed interpretation of the changes ongoing in Raman spectra. The room temperature structure contains three independent TiF_6 octahedra. One of them denoted as $Ti3F_6$, which is orientationally disordered between four positions, becomes ordered in low temperature (cubic) phase, while two other octahedra $Ti1F_6$ and $Ti2F_6$ rotate relatively to the initial orientation by a large angle. This means that a reconstructive phase transition takes place at 292.5 K. Additionally, the number of hydrogen bonds in *P*4/*mnc* is different from that in *Pa* $\overline{3}$ also indicating a significant reconstruction during the phase transition.

Low temperature phase demonstrates two peaks in the 600 cm^{-1} range which corresponds to fully symmetric TiF_6 stretching vibrations (see spectrum at 190 K in Fig.1). According to lattice dynamics calculations, the 614 cm^{-1} peak corresponds to a $Ti2F_6$ vibration while the 606 cm^{-1} peak is assigned to $Ti1F_6$. Internal ν_2 vibration of TiF_6 anion should be observed in the 450 cm^{-1} range; however, its intensity is usually small in the Raman spectra, and they are virtually not detected in our spectra. A single intense peak is observed at 282 cm^{-1}, which is assigned to ν_5 (F_{2g}) vibrations of $Ti2F_6$ and $Ti1F_6$ octahedra. The 200–250 cm^{-1} range contains translational vibrations of NH_4. Rocking vibrations of NH_4 appear in the range of 150 cm^{-1}. The intense Raman peak at 97 cm^{-1} is clearly seen in Fig.4; it is associated with the shortening of the hydrogen bond between NH_4 group and free fluorine atom (F7).[7] Visualization of this vibrational mode is shown in Fig. 5.

Spectral line at 67 cm^{-1} corresponds to rotary vibration TiF$_6$ octahedra and NH$_4$ displacement.[15] Further cooling down to 8 K leads to minor shift of Raman bands and to increase in their intensities.

Raman spectrum of the *P4/mnc* phase at 300 K (Fig.1, Table 1) contains two significantly wide bands assigned to TiF$_6$ vibrations, and also a Rayleigh wing of high intensity is observed. Translational and rocking vibrations of NH$_4$ are very weak. All these features indicate the structure disordering.

Further temperature increase above 360 K leads to yet another phase transition, and the structure of new high temperature phase is identified as *P4/mbm*.[7] The Rayleigh wing intensity is considerably decreased in this phase, and the 63 cm^{-1} line becomes more clear, that indicates less disorder of high temperature phase in comparison with the room temperature phase. Spectral lines of TiF$_6$ octahedra are somewhat shifted relative to their position at 300 K.

A single translationally independent tetrahedral NH$_4$ group of T$_d$ symmetry is present in the low temperature structure of (NH$_4$)$_3$TiF$_7$, and N–H bond length is equal to 0.9 Å (Fig. 6a).[7]

For T$_d$ group, a high frequency range of Raman spectra must contain four vibrations ν$_1$-ν$_4$.[16] However, the optimization of the initial geometry[7] gives the N–H bond lengths to be non-equal (Fig. 5b). This leads to the removal of degeneracy.

Spectral contour in the range of NH$_4$ bending vibrations in the range of 1300–1800 cm^{-1} at 8 K can be divided into at least ten peaks, while calculations predict twenty five modes, part of them, as can be deduced from Fig. 2b, are close enough to each other to be overlapped in the experimental spectra. Correspondingly, spectral contour in the NH$_4$ internal stretching vibrations at 3000–3350 cm^{-1} can be divided into at least six peaks, while calculations predict fifteen modes (Fig. 3b).

Room temperature structure contains two translationally independent NH$_4$ tetrahedra, therefore, as a result we must obtain eight vibrations, two normal vibrations for each spectral range, in accordance with the experiment. In the high temperature Raman spectrum, at 370 K,

(above the second phase transition), the lines remain sufficiently wide, that gives us the reason to assume the existence of two independent tetrahedra in this high temperature phase.

Conclusions

Raman spectra of $(NH_4)_3TiF_7$ were obtained for the first time in a wide range of frequencies (20–3400 cm^{-1}) and temperatures (8 – 370 K), which includes two phase transitions. It was experimentally established that the crystal structure of $Pa\overline{3}$ phase is stable down to 8 K, which is consistent with the results of the first-principle calculations.

The lines in the Raman spectra were identified and assigned by the types of vibrations of structural units. The mechanisms of phase transitions' implementation were established. It is shown that P4/mbm → P4/mnc is accompanied by disordering of TiF_6 octahedra evidenced by noticeable enlargement of the Rayleigh wing intensity.

P4/mnc→$Pa\overline{3}$ phase transition determined earlier as a reconstructive one is accompanied by ordering of TiF_6 octahedra and a symmetry lowering of NH_4 tetrahedra, the latter leads to the emergence of a large number of vibrational lines in the Raman spectra at low temperatures. Shortening of the bond lengths between the free fluorine atom and NH_4 group (N–H···F3, d(N···F) = 2.673 Å) leads to the emergence of mixed translational (NH_4+F_7) vibration, which is manifested (reflected) at 97 cm^{-1} below the temperature of reconstructive phase transition.

References

[1] S. S. Swendsen, Manufacture of titanium compounds, *US Patent* 2042434, **1936**.

[2] S. S. Swendsen, Treatment of titanium-bearing materials, *US Patent* 2042435, **1936.**

[3] G. L. Herwig, Upgrading titaniferous ores, *Australian Patent* 428758, **1972**.

[4] E. I. Mel'nichenko, I. G. Maslennikova, D. G. Epov, S. B. Bulanova, *Russ. J. Appl. Chem.* **1999**, *72*, 372–377.

[5] N. M. Laptash, I. G. Maslennikopva, L. N. Kurilenko, N. M. Mishchenko, *Russ. J. Inorg.* Chem. **2001**, *46*, 28–34.

[6] M. C. Marignac, *Ann. Mines* 1859, *15*, 221–290.

[7] M. Molokeev, S. V. Misjul, I. N. Flerov, N. M. Laptash, *Acta Cryst.* **2014**, *B70*, 924–931.

[8] S. V. Mel'nikova, E. I. Pogoreltsev, I. N. Flerov, N. M. Laptash, *J. Fluorine Chem.* **2014**, *165*, 14–19.

[9] E. I. Pogoreltsev, I. N. Flerov, A.V. Kartashev, E. V. Bogdanov, N. M. Laptash, *J. Fluorine Chem.* **2014**, *168*, 247–250.

[10] S. J. Clark, M. D. Segall, C. J. Pickard, P. J. Hasnip, M. J. Probert, K. Refson, M. C. Payne, *Zeitschrift fuer Kristallographie.* **2005**, *220*, 567–570.

[11] J. P. Perdew, A. Zunger, *Phys. Rev. B* **1981**, 23, 5048–5079.

[12] J. P. Perdew; K. Burke, M. Ernzerhof, *Phys. Rev. Lett.*, **1996**, 77, 3865-3868.

[13] H. J. Monkhorst, J. D. Pack, *Phys. Rev. B*, **1976**, 13, 5188–5192.

[14] P. Haas, F. Tran, P. Blaha, *Phys. Rev.* **2009**, *B 79*, 209902.

[15] W. von der Ohe, *J. Chem. Phys.* **1976**, *65*, 3575–3585.

[16] K. Nakamoto, Infrared and Raman Spectra of Inorganic and Coordination Compounds, 6th edn. Wiley, New York etc., 2009.
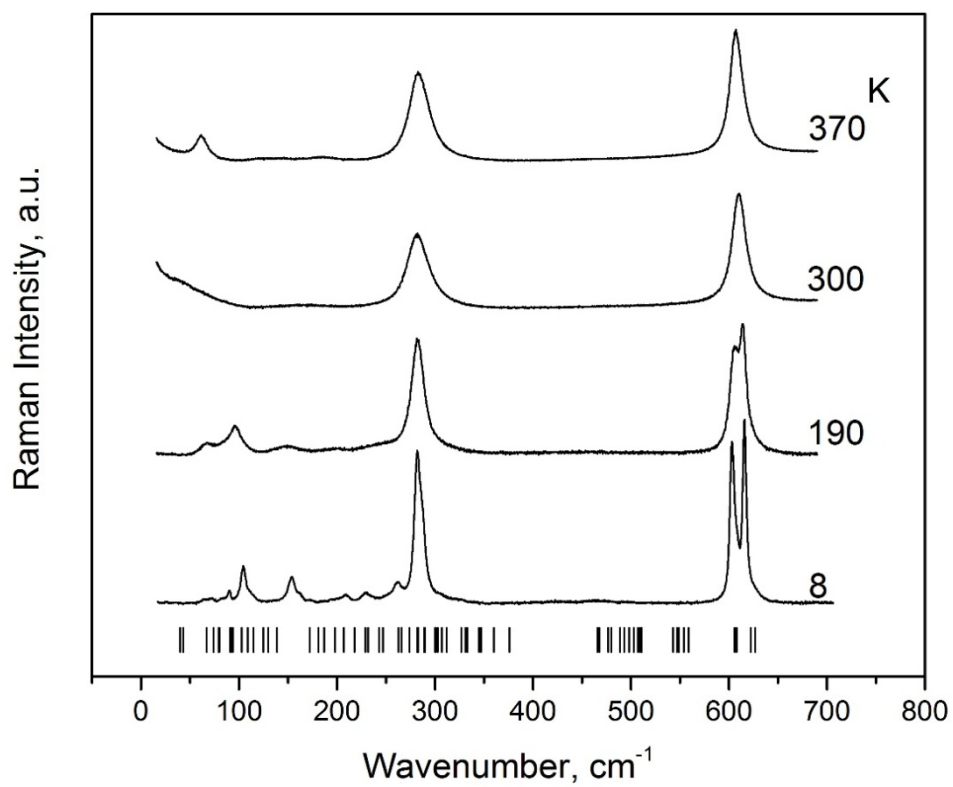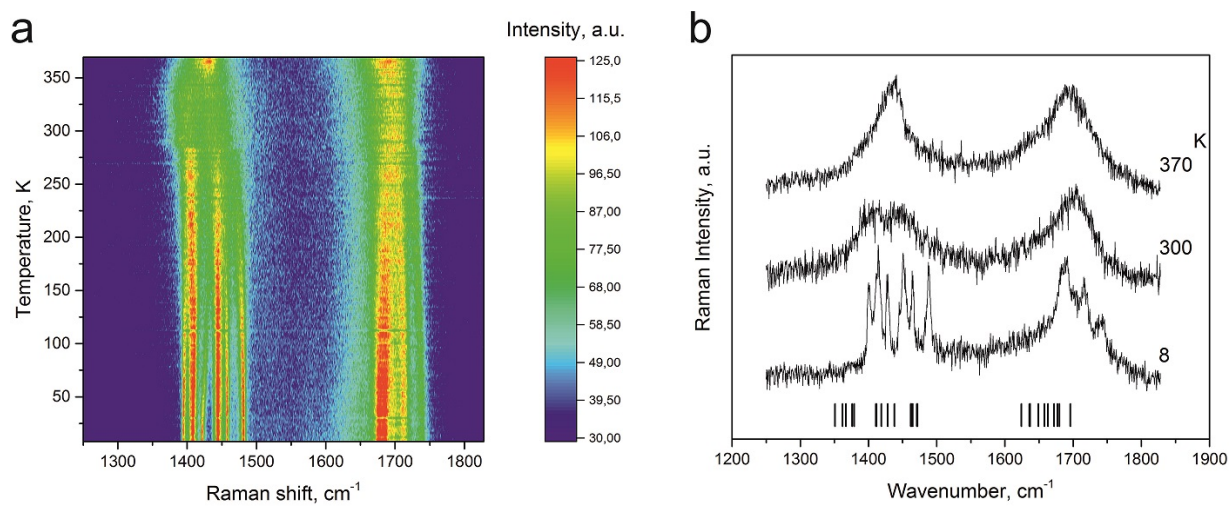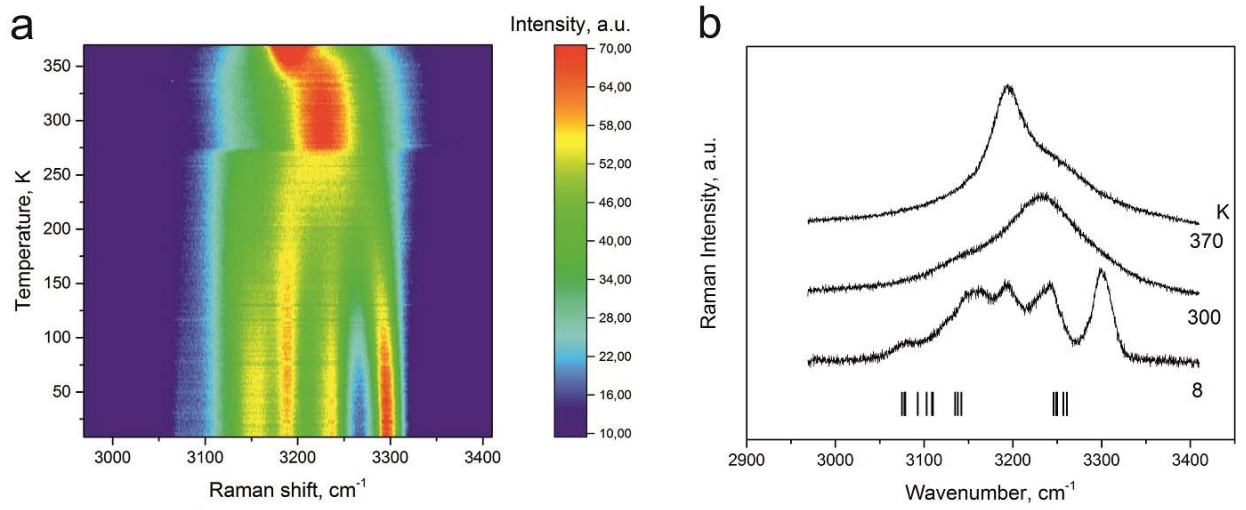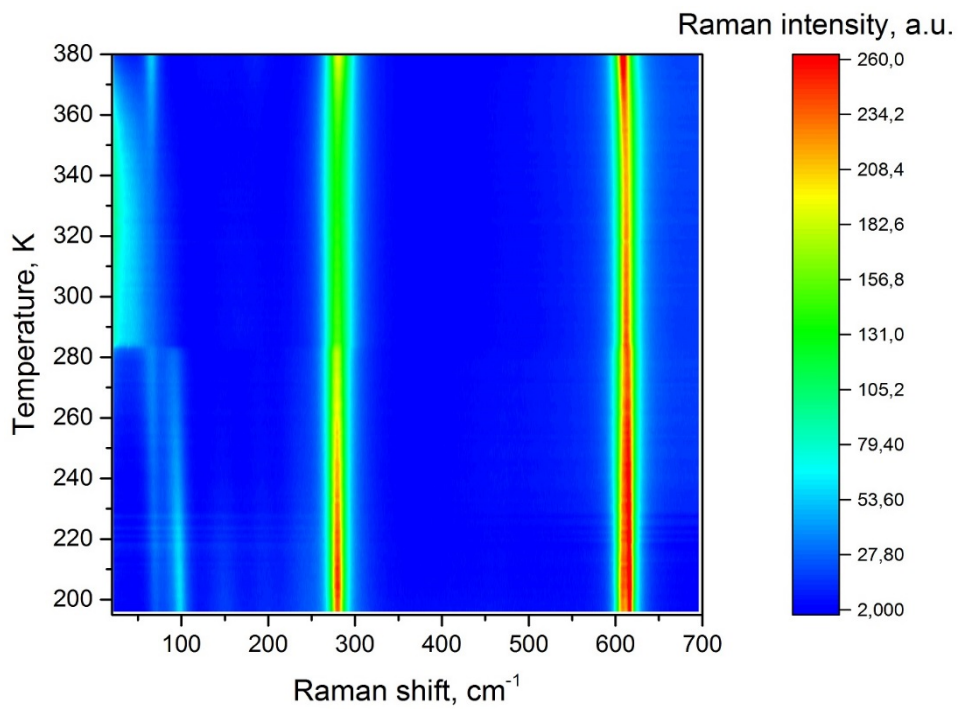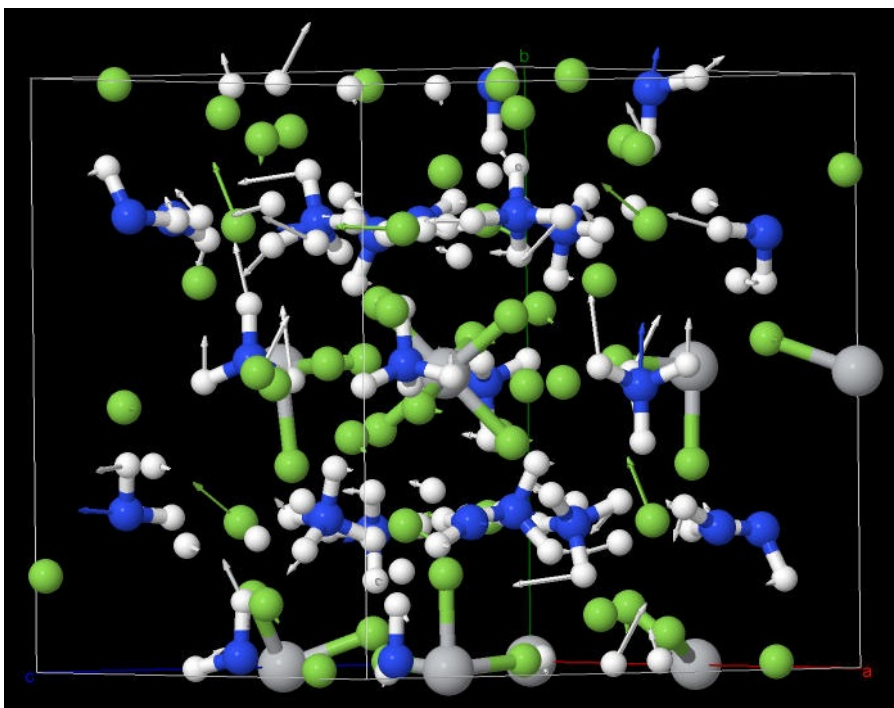
Figures

Fig.1

Fig.2

Fig.3

Fig.4

Fig.5
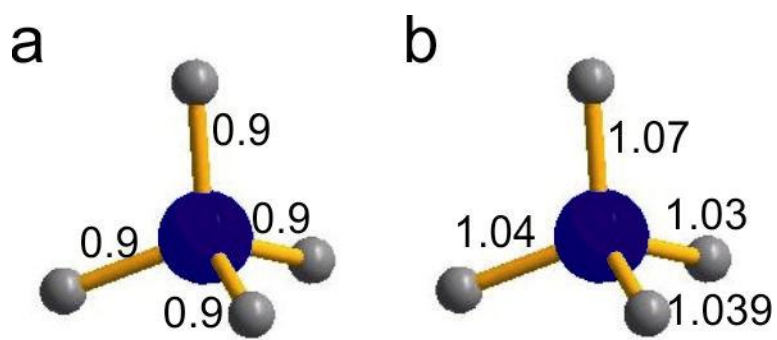

Fig.6

Captions to Figures

Figure 1. Raman spectra of $(NH_4)_3TiF_7$ in the range of TiF_6 and lattice vibrations at different temperatures. DFT-calculated Raman-active zone-center phonon frequencies are shown by vertical ticks.

Figure 2. Raman intensity maps (a) and temperature transformation (b) of bending vibrations of ammonium ions in $(NH_4)_3TiF_7$. DFT-calculated Raman-active zone-center phonon frequencies are shown by vertical ticks.

Figure 3. Raman intensity maps (a) and temperature transformation (b) of stretching vibrations of ammonium ions in $(NH_4)_3TiF_7$. DFT-calculated Raman-active zone-center phonon frequencies are shown by vertical ticks.

Figure 4. Raman intensity maps of $(NH_4)_3TiF_7$ spectra in the region of 20–700 cm^{-1}.

Figure 5. Simulated mixed translation of NH_4 groups and free fluorine atom (F7) related to Raman peak observed at 97 cm^{-1}.

Figure 6. Interatomic distances in the NH_4 tetrahedron: a) XRD data, $T = 143K$[7], b) DFT calculation.

Table 1. Experimental Raman wavenumbers of different phases of $(NH_4)_3TiF_7$ and their assignments

8 K	190 K	300 K	370 K	Description
3077, 3128, 3157, 3192, 3240, 3299	3077, 3153, 3194, 3240, 3286	3142, 3232	3196, 3258	ν_1, ν_3 NH_4
1686, 1716, 1742	1690, 1712, 1734	1700	1692	ν_2 NH_4
1400, 1414, 1427, 1446, 1450, 1464, 1488	1409, 1452, 1481,	1405, 1448	1436	ν_4 NH_4
603 615	606 614	610	606	ν_1 TiF_6
287, 281	282	282	283	ν_5 TiF_6
261, 230 209	243 201		186	Transl NH_4
153, 163,	150		124	Rocking NH_4
104, 90	97			Transl (NH_4 + F7)
64, 72	67		62	Transl NH_4 + Rotation TiF_6

Acknowledgment